

Organotin biocides. X.* Synthesis, structure and biocidal activity of organotin derivatives of 2-mercaptobenzothiazole, 2-mercaptobenzoxazole and 2-mercaptobenzimidazole

K C Molloy†, T G Purcell†, D Cunningham‡, P McCardle‡ and T Higgins§

†School of Chemistry, University of Bath, Claverton Down, Bath BA2 7AY, UK, ‡Department of Chemistry, University College, Galway, Ireland, §Department of Physical Sciences, Regional Technical College, Galway, Ireland

Received 28 August 1986 Accepted 23 June 1986

Ten organotin derivatives of 2-mercaptobenzothiazole (Hmbt), 2-mercaptobenzoxazole (Hmbo) and 2-mercaptobenzimidazole (Hmbi) have been synthesised and their structures characterised by spectroscopic methods. Triorganotin derivatives are all S-bonded to the ligand and four-coordinate at tin except $\text{Bu}_3\text{Sn}(\text{mbo})$ which is a five-coordinate *trans*- ONSnR_3 polymer at 78 K. The crystal structure of $\text{Cy}_3\text{Sn}(\text{mbt})$ has been determined and confirms the tetrahedral geometry at tin. $\text{Bu}_2\text{Sn}(\text{mbt})_2$ is weakly six-coordinate by N,S chelating ligands. Biocidal activity patterns are presented for $\text{Cy}_3\text{Sn}(\text{mbt})$, $\text{Ph}_3\text{Sn}(\text{mbt})$ and $\text{Ph}_3\text{Sn}(\text{mbo})$.

Keywords: Organotin, Mössbauer, X-ray, structure, biocides

INTRODUCTION

Metallo-complexes of 2-mercaptobenzothiazole (Hmbt) and the related heterocycles 2-mercaptobenzoxazole (Hmbo) and 2-mercaptobenzimidazole (Hmbi) have proved a fertile area for study over a number of years, stimulated both by the diversity of their commercial applications and the richness of their structural chemistry. Zinc complexes of mercaptobenzothiazole have been implicated in the acceleration of rubber vulcanisation, and the structures of both zinc and cadmium complexes of this ligand have been thoroughly investi-

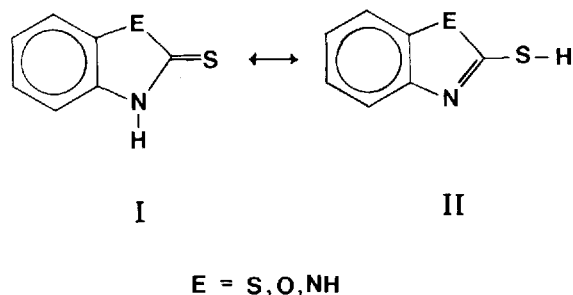
gated.¹⁻³ As part of a study of the protective action of organic corrosion inhibitors towards metals the structures of $\text{Ru}_2(\text{mbt})_2(\text{py})_2(\text{CO})_4$,⁴ $\text{Ru}(\text{mbt})_2(\text{py})_2(\text{CO})_2$ ⁵ and the sulphur-bridged dimer $[\text{Re}(\text{mbt})(\text{CO})_3]_2$ ⁶ have been reported. Benzimidazoles exhibit similar corrosion inhibition properties.^{7,8} Moreover, these ligands (but particularly Hmbt) are parents to a class of organic and metal-organic compounds which have known fungicidal activity, which in the case of Hmbt and its derivatives possibly arises from opening of the thiazole ring to yield toxic dithiocarbamates.⁹

All three mercaptans can exist in two tautomeric forms (I,II) but crystallographic studies of Hmbt¹⁰ and Hmbi¹¹ show that the thione form (I) is preferred, at least in the solid state. In addition, these ligands have a catholic capacity for binding metal ions,¹²⁻¹⁷ and at least four bonding modes between ligand and metal are conceivable (Fig. 1). Coordination by the exocyclic sulphur only (Fig. 1a) is found in $\text{Ru}(\text{mbt})_2(\text{py})_2(\text{CO})_2$ ⁵ and by the endocyclic nitrogen only (Fig. 1b) in both $[\text{Zn}(\text{S}_2\text{CNMe}_2)_2(\text{mbt})]^-$ and $[\text{Zn}(\text{S}_2\text{CNMe}_2)(\text{mbt})_2]^-$ while heterocycles with each of these linkages are found in $[\text{Zn}(\text{mbt})_3(\text{H}_2\text{O})]^-$.² Chelation by S and E atoms (Fig. 1c) is to our knowledge unknown, but N,S chelation (Fig. 1d) is common, e.g. $\text{Co}(\text{mbt})_2(\text{py})_2$,¹⁸ $[\text{Cd}(\text{mbt})_3]^-$.³ In addition, bridging rather than chelation and/or distortions from regular geometry are possible.

Our interest in the biocidal nature of organotin compounds¹⁹ has prompted us to investigate in some detail the synthesis, structures and activity patterns for derivatives of the titled heterocycles,

*For Part IX see ref. 19.

which we report herein. Varying degrees of fungicidal activity have been noted by other workers²⁰⁻²² for R_3SnL ($R = n\text{-Bu, Ph; } L = \text{mbt, mbo}$) and spectroscopic data for $Me_3Sn(\text{mbt})$, $Bu_3Sn(\text{mbt})$, $Bu_2Sn(\text{mbt})_2$ reported.^{23,24}



EXPERIMENTAL

Organotin reagents and the title heterocycles were of commercial origin and were used without further purification. Solvents were dried by conventional methods prior to use. Spectra were recorded using the following instruments: Perkin Elmer 599b (infrared), Perkin Elmer R12B or R24B (1H n.m.r.), Jeol FX60Q (^{119}Sn n.m.r.), V.G. 70-70E (mass spectra). Details of our Mössbauer spectrometer and related procedures are given elsewhere.²⁵ Organotin derivatives of the three heterocycles were prepared from either the organotin oxide or hydroxide and the free ligand or, in the case of $Me_3Sn(\text{mbt})$, from the tin halide and the sodium salt of the ligand. The routes are typified by the two detailed syntheses given below. Further details and analytical data are given in Table 1.

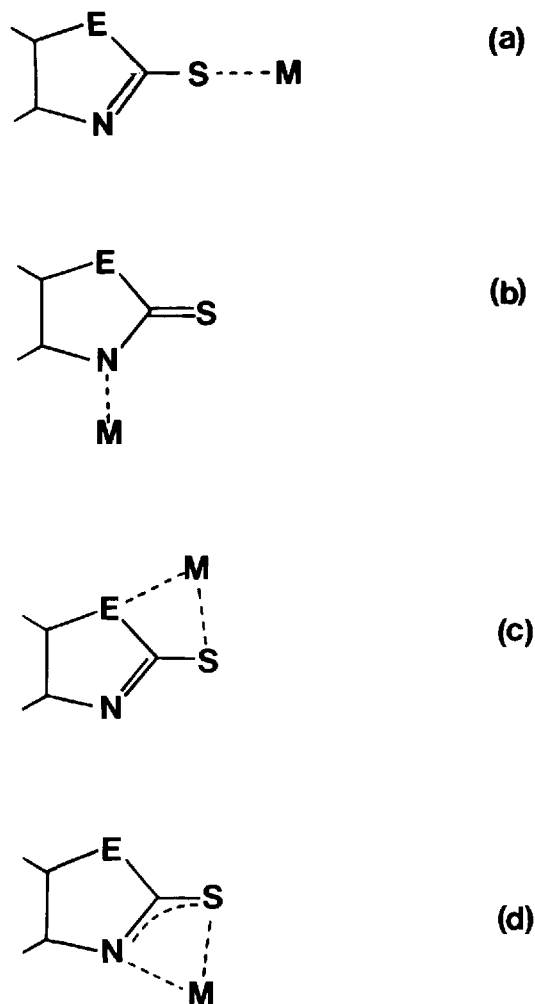


Figure 1 Possible modes of coordination of the title heterocycles to metals (M). E = S (mbt), O (mbo) or NH (mbi).

Table 1 Physical data^a

Compound	Yield(%)	m.p.(°C)	C ^b	H ^b	N ^b
$Me_3Sn(\text{mbt})$	28 ^c	oil	36.21(36.28)	3.95(3.96)	4.18(4.23)
$Bu_3Sn(\text{mbt})$	41 ^c	oil	50.00(50.02)	7.09(6.85)	3.00(3.07)
$Cy_3Sn(\text{mbt})$	80 ^d	72	56.36(56.19)	6.56(6.80)	2.59(2.62)
$Bz_3Sn(\text{mbt})$	79 ^c	80-81	59.96(60.10)	4.80(4.51)	2.56(2.50)
$Ph_3Sn(\text{mbt})$	40 ^e	92-93	58.14(58.16)	3.52(3.71)	2.66(2.71)
$Bu_2Sn(\text{mbt})_2$	32 ^c	68-70 ^f	45.03(46.65)	5.13(4.64)	4.51(4.95)
$Bu_3Sn(\text{mbo})$	52 ^c	oil	51.60(51.84)	7.25(7.10)	3.06(3.18)
$Cy_3Sn(\text{mbo})$	40 ^d	46-47	56.59(56.93)	7.11(7.37)	2.48(2.77)
$Ph_3Sn(\text{mbo})$	50 ^e	96-98	60.03(59.91)	3.81(3.82)	2.69(2.72)
$Cy_3Sn(\text{mbi})$	32 ^h	165-166	57.80(58.04)	7.10(7.04)	5.49(5.42)

^aAbbreviations: Bu = $n\text{-C}_4\text{H}_9$, Cy = cyclo- C_6H_{11} , Bz = $\text{C}_6\text{H}_5\text{CH}_2$, ^bCalculated values in parentheses (%). ^cRecrystallised from EtOH, ^dRecrystallised from $\text{Et}_2\text{O}/\text{MeOH}$, ^eRecrystallised from $\text{CHCl}_3/\text{EtOH}$, ^fLit: 75.7-77°C, ^gRecrystallised from $\text{CH}_2\text{Cl}_2/\text{EtOH}$, ^hRecrystallised from $\text{C}_6\text{H}_5\text{CH}_3$.

Synthesis of S-(tricyclohexylstannyl)-2-mercaptobenzothiazole

Tricyclohexyltin hydroxide (3.45 g, 9.0 mmol) and Hmbt (1.5 g, 9.0 mmol) were refluxed in toluene for 2 h, and water produced during the course of the reaction removed using a Dean and Stark trap. After cooling, the solution was filtered and the filtrate evaporated to dryness to yield a yellow oil. Trituration with a small volume of cold ethanol induced solidification, and the resulting solid was recrystallised from ether/ethanol (1:2) to yield the desired compound (3.85 g, 80%).

Synthesis of S-(trimethylstannyl)-2-mercaptobenzothiazole

Hmbt (2.0 g, 12.0 mmol) was dissolved in an ethanolic solution (15 cm³) containing sodium (0.22 g, 13 mmol). Trimethyltin chloride (2.4 g, 12.0 mmol) in ethanol (10 cm³) was added, and the mixture refluxed for 2 h. The solution was evaporated to dryness and the resulting oil dissolved in petroleum ether and filtered to remove NaCl and any unreacted ligand. The solvent was again removed in vacuo, and the oily product purified by repeated dissolution in hot ethanol, reprecipitating upon cooling and decanting off the supernatant liquid. Prolonged drying under vacuum removed the last traces of solvent, to yield the product as an analytically pure oil (1.11 g, 28%).

X-ray crystal structure of (C₆H₁₁)₃Sn(mbt)

Suitable crystals for x-ray analysis were grown from an ether/methanol mixture.

Crystal data: C₂₅H₃₇NS₂Sn, MW = 535.43, triclinic P $\bar{1}$, $a = 13.0336$, $b = 11.1264$, $c = 10.1878$ Å, $\alpha = 62.49^\circ$, $\beta = 94.79^\circ$, $\gamma = 95.51^\circ$, $V = 1302.02$ Å³, $Z = 2$, $\rho_{\text{calc}} = 1.362$ g cm⁻³, $F(000) = 522$, $\mu(\text{Mo-K}\alpha) = 10.52$ cm⁻¹.

Data collection was carried out at room temperature on a Hilger-Watts Y290 four-circle automatic diffractometer using Mo-K α radiation. 3047 reflections were measured, of which 2377 had $I > 3\sigma(I)$ and were considered observed. The structure was solved by direct methods using MULTAN²⁶ and refined using the SHELX program suite.²⁷ Final values for 2377 observed reflections are $R = 0.0542$ and $R_w = 0.0600$. Atomic scattering factors for non-hydrogen and hydrogen atoms were taken from Cromer and Mann²⁸ and Stewart et al.²⁹ respectively. Anomalous disper-

sion corrections for non-hydrogen atoms were taken from Cromer and Liberman.³⁰ Final positional parameters for non-hydrogen atoms and bond distances and angles involving these atoms are given in Tables 2 and 3. Positional parameters for hydrogen atoms and complete thermal data for all atoms are available upon request from the authors.

Biocidal testing

Ph₃Sn(mbo), Ph₃Sn(mbt) and Cy₃Sn(mbt) (500 µg g⁻¹; ppm) were tested against *Tetranychus urticae* on French bean, *Nilaparvata lugens* on rice, *Chilo partellus* on rape and *Musca domestica* (sample in plastic cup) and their effectiveness measured on a 0–9 scale after between 1 and 6 days.

Against *Botrytis cinerea*, the compound was incorporated into PDA plates at 5 µg g⁻¹. Organisms were inoculated as 7 day old spores suspensions or as mycelial plugs. Incubation was at 19 or 25°C. Disease assessment was made on a 0–4 scale after 2 days.

In the cases of *Puccinia recondita* (host: wheat), *Venturia inaequalis* (apple), *Plasmopara viticola* (vine), *Pyricularia oryzae* (rice) and *Cercospora arachidicola* (peanut), the test compound was applied as a combined protectant spray and systemic root drench at the appropriate concentration level 1 or 2 days before inoculating young plants. Disease assessments (0–4 scale) were made 5–12 days after inoculation.

Full details of testing procedures towards *Tetranychus urticae*, *Plasmopara viticola* and *Phytophthora infestans* are given elsewhere.³¹

DISCUSSION

Synthesis and spectroscopy

Organotin derivatives of the three 2-mercapto-substituted heterocycles are straightforwardly prepared by the reaction of an organotin oxide or hydroxide with the free ligands (Eqns 1, 2, 3) or by a metathesis reaction involving an organotin chloride and the sodium salt of the ligand (Eqn 4).

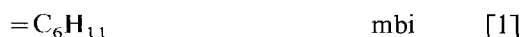
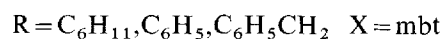
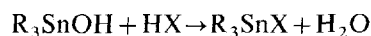
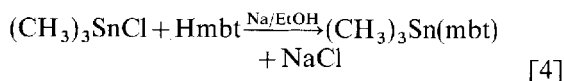
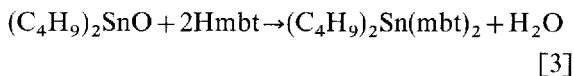
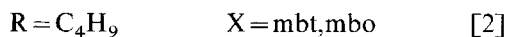
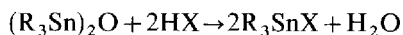


Table 2 Final fractional positional and thermal parameters for non-hydrogen atoms in (C₆H₁₁)₃Sn(mbt)

Atom	x	y	z	U _{iso} or U ₁₁	U ₂₂	U ₃₃	U ₂₃	U ₁₃	U ₁₂
Sn	0.27094(5)	0.01442(6)	0.27575(6)	0.0535(4)	0.0534(4)	0.0480(4)	−0.0222(3)	−0.0053(3)	0.0006(3)
S(1)	0.1192(2)	0.0274(3)	0.1081(3)	0.071(2)	0.062(1)	0.067(2)	−0.028(1)	−0.019(1)	0.002(1)
S(2)	0.0291(2)	0.2845(3)	−0.1213(3)	0.082(2)	0.081(2)	0.077(2)	−0.033(1)	−0.029(1)	0.021(1)
N	0.1718(6)	0.2801(8)	0.0718(9)	0.066(2)	—	—	—	—	—
C(1)	0.1151(7)	0.2034(10)	0.0271(10)	0.061(2)	—	—	—	—	—
C(2)	0.0757(8)	0.4381(11)	−0.1224(11)	0.072(3)	—	—	—	—	—
C(3)	0.0418(10)	0.5685(13)	−0.2148(14)	0.091(3)	—	—	—	—	—
C(4)	0.0884(10)	0.6694(15)	−0.1876(15)	0.099(4)	—	—	—	—	—
C(5)	0.1625(10)	0.6477(14)	−0.0792(15)	0.100(4)	—	—	—	—	—
C(6)	0.1964(9)	0.5208(12)	0.0098(13)	0.083(3)	—	—	—	—	—
C(7)	0.1491(8)	0.4122(11)	−0.0124(11)	0.070(3)	—	—	—	—	—
C(8)	0.2827(9)	−0.2046(11)	0.3716(13)	0.081(3)	—	—	—	—	—
C(9)	0.3780(10)	−0.2504(13)	0.4736(14)	0.091(3)	—	—	—	—	—
C(10)	0.3892(12)	−0.4016(16)	0.5391(19)	0.119(5)	—	—	—	—	—
C(11)	0.2890(15)	−0.4820(22)	0.5920(23)	0.158(7)	—	—	—	—	—
C(12)	0.2030(14)	−0.4365(17)	0.4840(20)	0.139(6)	—	—	—	—	—
C(13)	0.1883(12)	−0.2877(15)	0.4327(18)	0.117(5)	—	—	—	—	—
C(14)	0.2431(8)	0.0895(10)	0.4290(11)	0.069(3)	—	—	—	—	—
C(15)	0.1328(9)	0.0901(12)	0.4581(13)	0.079(3)	—	—	—	—	—
C(16)	0.1207(11)	0.1509(13)	0.5626(14)	0.095(4)	—	—	—	—	—
C(17)	0.1887(11)	0.0906(15)	0.7010(16)	0.109(4)	—	—	—	—	—
C(18)	0.2963(11)	0.0876(15)	0.6743(16)	0.106(4)	—	—	—	—	—
C(19)	0.3086(10)	0.0272(12)	0.5697(13)	0.088(3)	—	—	—	—	—
C(20)	0.4061(8)	0.1160(10)	0.1483(10)	0.063(2)	—	—	—	—	—
C(21)	0.3912(9)	0.1549(12)	−0.0122(12)	0.081(3)	—	—	—	—	—
C(22)	0.4854(10)	0.2229(13)	−0.0997(15)	0.095(4)	—	—	—	—	—
C(23)	0.5309(11)	0.3332(14)	−0.0724(14)	0.097(4)	—	—	—	—	—
C(24)	0.5479(10)	0.2981(13)	0.0884(13)	0.093(3)	—	—	—	—	—
C(25)	0.4497(9)	0.2360(12)	0.1710(13)	0.081(3)	—	—	—	—	—



The compounds are stable crystalline solids, except for Me₃Sn(mbt) and the two tributyltin derivatives which are oils. Bu₂Sn(mbt)₂ contains traces of Bu₂SnO (its precursor) as indicated by Mössbauer spectroscopy, and from which it is difficult to completely separate.

Mass spectral data confirm the composition of the organotin heterocycles, although under EI conditions only Ph₃Sn(mbt) and Ph₃Sn(mbo) show parent ions. The highest observable fragment for the remaining compounds corresponds

to R₂SnL⁺ and except for (C₆H₅CH₂)₃Sn(mbt), this is the most intense ion observed in the respective spectra. [P+H]⁺ fragments are seen in the CI (iso-butene) spectra of Bu₃Sn(mbt), Me₃Sn(mbt) and Cy₃Sn(mbo) along with ions of masses [P+57]⁺ (C₄H₉) and [P+41]⁺, [P+43]⁺ (C₃H₅, C₃H₇) resulting from interactions with the ionising gas. This latter finding is in contrast to the absence of similar combination ions in the CI spectra of organotinins as noted by Fish et al.³² More surprisingly, the CI spectra of Bu₃Sn(mbt) and Me₃Sn(mbt) also contain ditin fragments, although no such species are seen under EI conditions. For example, we assign fragments of masses 748 in the spectrum of the butyltin compound and 647, 617 in the spectrum of Me₃Sn(mbt) to (Bu₃Sn)₂C₇H₄NS₂, Me₅Sn₂(C₇H₄NS₂)₂ and Me₃Sn₂(C₇H₄NS₂)₂ respectively. We can, however, find no justification in any of the complementary spectra of these compounds to assign oligomeric or polymeric structures, and thus conclude that the appearance of such ions is an

Table 3 Intramolecular bond distances (Å) and angles (°) for (C₆H₁₁)₃Sn(mbt)

Distances			
Sn—S(1)	2.472(2)	C(14)—C(15)	1.494(15)
Sn—N	3.055(8)	C(15)—C(16)	1.526(16)
Sn—C(8)	2.183(11)	C(16)—C(17)	1.502(18)
Sn—C(14)	2.150(10)	C(17)—C(18)	1.457(19)
Sn—C(20)	2.170(9)	C(18)—C(19)	1.529(18)
—	—	C(19)—C(14)	1.502(15)
C(1)—S(1)	1.743(10)	—	—
C(1)—N	1.290(12)	C(20)—C(21)	1.486(14)
C(1)—S	1.734(10)	C(21)—C(22)	1.502(16)
C(7)—N	1.364(13)	C(22)—C(23)	1.443(16)
C(2)—S(2)	1.753(11)	C(23)—C(24)	1.500(17)
C(2)—C(3)	1.407(16)	C(24)—C(25)	1.515(16)
C(3)—C(4)	1.355(17)	C(25)—C(20)	1.509(14)
C(4)—C(5)	1.353(18)	—	—
C(5)—C(6)	1.372(17)	C(8)—C(9)	1.515(17)
C(6)—C(7)	1.406(15)	C(9)—C(10)	1.514(19)
C(2)—C(7)	1.352(15)	C(10)—C(11)	1.498(22)
—	—	C(11)—C(12)	1.453(24)
—	—	C(12)—C(13)	1.515(21)
—	—	C(13)—C(8)	1.461(17)
Angles			
C(8)—Sn—C(20)	108.6(4)	C(8)—C(9)—C(10)	112.9(11)
C(14)—Sn—C(8)	115.7(4)	C(9)—C(10)—C(11)	111.9(14)
C(20)—Sn—C(14)	112.4(4)	C(10)—C(11)—C(12)	114.3(17)
C(8)—Sn—N	153.6(3)	C(11)—C(12)—C(13)	110.9(16)
C(14)—Sn—N	78.3(3)	C(12)—C(13)—C(8)	116.8(13)
C(20)—Sn—N	83.8(3)	C(13)—C(8)—C(9)	114.2(11)
C(14)—Sn—S(1)	112.3(3)	—	—
C(8)—Sn—S(1)	96.6(3)	C(14)—C(15)—C(16)	112.4(9)
C(20)—Sn—S(1)	110.2(3)	C(15)—C(16)—C(17)	112.8(11)
—	—	C(16)—C(17)—C(18)	114.1(13)
C(1)—S(1)—Sn	95.7(3)	C(17)—C(18)—C(19)	112.7(12)
C(1)—N—Sn	82.8(6)	C(18)—C(19)—C(14)	112.7(12)
N—C(1)—S(1)	124.1(8)	C(19)—C(14)—C(15)	113.3(10)
S(2)—C(1)—S(1)	119.7(6)	—	—
C(1)—N—C(7)	109.9(9)	C(20)—C(21)—C(22)	110.7(9)
N—C(7)—C(2)	117.1(1)	C(21)—C(22)—C(23)	114.1(10)
C(7)—C(2)—S(1)	108.8(8)	C(22)—C(23)—C(24)	112.5(11)
C(2)—S(2)—C(1)	87.9(5)	C(23)—C(24)—C(25)	114.5(11)
C(2)—C(3)—C(4)	115.5(13)	C(24)—C(25)—C(20)	111.1(11)
C(3)—C(4)—C(5)	122.9(15)	C(25)—C(20)—C(21)	111.1(9)
C(4)—C(5)—C(6)	121.7(14)	—	—
C(5)—C(6)—C(7)	117.6(12)	—	—
C(6)—C(7)—C(2)	119.0(11)	—	—
C(7)—C(2)—C(3)	123.4(11)	—	—

artefact of the conditions prevailing in the spectrometer. Full mass spectral data are available upon request from the authors.

Infrared data (Table 4) are complex, due to both the richness of the spectra and in view of the fact that most absorptions do not correspond to simple 'one-bond' vibrations but result from coupling of two or more motions. Bands relating to the thioamide group ($\text{S}=\text{C}-\text{NH}$ or its tautomeric form) and those bands containing contributions from $\nu(\text{C}-\text{S}_{\text{exo}})$ are assigned by comparison with literature values.³³ Structural inferences based upon these data are generally ambiguous. For example, a band at ca. 1595 cm^{-1} in Hmbt has been assigned by several workers to a pure $\nu(\text{C}=\text{N})$ and occurs at 1616 cm^{-1} and 1620 cm^{-1} in Hmbo and Hmbi respectively. Upon coordination to transition metals this band moves to $1565\text{--}1590\text{ cm}^{-1}$ and weakens in intensity, and this has been taken as evidence for N-to-metal coordination.^{12,16} However, in the complex $\text{Ru}(\text{mbt})_2(\text{py})_2(\text{CO})_2$ in which mbt is bonded to ruthenium by the exocyclic sulphur only, a band assigned to $\nu(\text{C}=\text{N})$ occurs at 1565 cm^{-1} . Indeed, in this complex the $\text{C}=\text{N}$ bond is shorter than in Hmbt! The structural conclusions which we draw from our data are therefore limited and cautious. Firstly, for $\text{Me}_3\text{Sn}(\text{mbt})$ and $\text{Bz}_3\text{Sn}(\text{mbt})$ bands assignable to $\nu_{\text{asym, symm}}(\text{Sn}-\text{C})$ are observed, indicating a non-planar $[\text{SnC}_3]$ moiety. Secondly, despite the presence of ligand vibrations in the $300\text{--}400\text{ cm}^{-1}$ region, new bands appear upon coordination to tin, and arise from $\nu(\text{Sn}-\text{S})$. In a limited number of cases we have been able to assign this vibration with some confidence.

Finally, in the case of $\text{Cy}_3\text{Sn}(\text{mbi})$ (and only in this case) $\nu(\text{N}-\text{H})$ remains after complexation to tin, arising from the second $\text{N}-\text{H}$ group in the ligand. This band is broad and appears at lower frequency than Hmbi, and most probably arises from $\text{N}-\text{H}\cdots\text{N}$ hydrogen bonding as bifurcated $\text{NH}\cdots\text{S}\cdots\text{HN}$ hydrogen bonding occurs in Hmbi.¹¹

^1H and ^{119}Sn nmr data are given in Table 5. $^2\text{J}(^{119}\text{Sn}-\text{C}-^1\text{H})$ for $\text{Me}_3\text{Sn}(\text{mbt})$ (59 Hz) and $\text{Bz}_3\text{Sn}(\text{mbt})$ (65 Hz) are consistent with data for tetrahedral organotin mercaptides $\text{Me}_3\text{SnSC}_6\text{H}_4\text{X}-p$ ($\text{X} = \text{H}, \text{Me}, \text{Bu}, \text{Cl}$ etc.) of 56.7 Hz ³⁴ and the value for the trimethyltin compound is similar to that found by Domazetis et al.²⁴ of 63 Hz. However, similar coupling constants also arise from five-coordinate, *cis*- XYSnR_3 geometries [e.g. $\text{Me}_3\text{Sn}(\text{ON. Ph. CO. Ph})$ 54 Hz,³⁵ a structure which is also plausible from the non-planarity of the $[\text{SnC}_3]$ unit as indicated by IR data (vide supra). In the case of the three tricyclohexyltin compounds $\delta\ ^{119}\text{Sn}$ occurs ca. 30 ppm and is clearly due to a four-coordinated tin (e.g. Cy_3SnBr 69.1 ppm; Cy_3SnI 56.7 ppm), resonances due to tin in higher coordination environments occurring at higher field, e.g. $\text{Cy}_3\text{Sn}(\text{tropolonate})$ -62.8 ppm .³⁶ $^1\text{J}(^{119}\text{Sn}-^{13}\text{C})$ data for $\text{Bu}_3\text{Sn}(\text{mbt})$ ²⁴ are also consistent with a tetrahedral coordination at tin, and on the basis of this collective solution phase data we assign a coordination number of four at tin all cases.

In the solid state, Mössbauer Quadrupole Splitting (QS) data (Table 5) provide evidence for the coordination environment of the Mössbauer active nucleus, in this case tin. Data for all the tri-

Table 4 Selected infrared data (cm^{-1})

Compound	$\nu(\text{N}-\text{H})$	Thioamide bands	$\nu(\text{C}=\text{S})$ containing bands	$\nu_{\text{asym, sym}}(\text{Sn}-\text{C})$	$\nu(\text{Sn}-\text{S})$
Hmbt	3105 m	1595 m, 1597 s, 1282 m	1032 s, 1012 s, 602 s, 526 w, 391 w	—	—
$\text{Me}_3\text{Sn}(\text{mbt})^a$	—	1560 vw, 1480 sh, 1275 w	998 s, 980 m, 602 vw, 515 m	540 s, 513 m	396 sh
$\text{Bu}_3\text{Sn}(\text{mbt})$	—	1560 vw, 1465 m, 1278 w	995 s, 982 s, 602 w	—	—
$\text{Cy}_3\text{Sn}(\text{mbt})$	—	1555 w, 1466, 1280 w	1001 s, 995 s, 601 vw, 505 vw	—	398 sh
$\text{Bz}_3\text{Sn}(\text{mbt})$	—	1560 vw, 1466 sh, 1280 w	1008 s, 1002 s, 604 vw, 510 vw	570 vw, 550 vw	400 sh
$\text{Ph}_3\text{Sn}(\text{mbt})$	—	1580 vw, 1470 sh, 1270 w	1008 s, 993 s, 600 vw, 505 vw	—	—
$\text{Bu}_3\text{Sn}(\text{mbt})_2$	—	1555 vw, 1462 sh, 1270 w	1005 s, 1000 s, 602 w, 505 vw	—	—
Hmbo	3225 br	1616 m, 1500 s, 1280 m	1410 s, 813 m, 675 m, 480 m, 430 s	—	—
$\text{Bu}_3\text{Sn}(\text{mbo})$	—	1600 vw, 1480s, 1275 w	810 m, 419 m	—	—
$\text{Cy}_3\text{Sn}(\text{mbo})$	—	1580 vw, 1480 sh, 1272 w	813 m, 675 vw, 422 m	—	392 w
$\text{Ph}_3\text{Sn}(\text{mbo})$	—	1600 vw, 1490 s, 1280 vw	810 m, 665 vw, 417 m	—	397 w
Hmbi	3155	1620 m, 1510 s, 1260 m, 705 br	658 m, 598 s, 480 m, 418 m	—	—
$\text{Cy}_3\text{Sn}(\text{mbi})$	3135br ^b	1615 vw, 1515 w, 1270 s	658 w, 600 w, 479 w, 414 m	—	—

^a $\rho(\text{Sn}-\text{Me})$: 780 cm^{-1} , ^bDiminished in intensity with respect to Hmbi, and corresponds to the remaining $\text{N}-\text{H}$ of the ligand.

Table 5 NMR and Mössbauer (78 K) spectroscopic data

Compound	$\delta\text{CH-Sn}^a$	$2J(^{119}\text{Sn-C-}^1\text{H})^b$	$\delta^{119}\text{Sn}^c$	IS ^d	QS ^e	$\Gamma_{1,2}^f$	$10^2 a(\text{K}^{-1})$
$\text{Me}_3\text{Sn(mbt)}$	0.65 ^g	59	—	1.35	2.40	1.03, 0.99	—
$\text{Bu}_3\text{Sn(mbt)}$	—	—	—	1.48	2.37	1.03, 1.02	—
$\text{Cy}_3\text{Sn(mbt)}$	—	—	37.7 ^h	1.54	2.22	0.94, 0.90	1.35 ⁱ
$\text{Bz}_3\text{Sn(mbt)}$	2.53 ^g	65	—	1.51	1.91	1.02, 0.97	—
$\text{Ph}_3\text{Sn(mbt)}$	—	—	—	1.31	1.80	0.86, 0.88	—
$\text{Bu}_2\text{Sn(mbt)}_2^j$	—	—	—	1.48	2.37	0.98, 0.92	—
$\text{Bu}_3\text{Sn(mbo)}$	—	—	—	1.28	3.26	1.17, 1.20	—
$\text{Cy}_3\text{Sn(mbo)}$	—	—	37.7 ^h	1.57	2.35	0.98, 0.99	—
$\text{Ph}_3\text{Sn(mbo)}$	—	—	—	1.34	2.03	0.99, 1.00	—
$\text{Cy}_3\text{Sn(mbi)}$	—	—	26.6 ^h	1.57	2.30	0.94, 0.95	1.68 ^k

^appm relative to Me_4Si , ^bHz, ^cppm relative to Me_4Sn , ^d $\pm 0.02 \text{ mm s}^{-1}$, ^e $\pm 0.04 \text{ mm s}^{-1}$, ^fFull width at half height, ^g CDCl_3 solution, ^hToluene solution, ⁱCorrelation coefficient = $-0.999(78\text{--}140 \text{ K}; 5 \text{ pts})$, ^jMössbauer spectrum also contains a second doublet $\text{IS} = 1.00$, $\text{QS} = 2.04 \text{ mm s}^{-1}$, ^kCorrelation coefficient = $-0.998(78\text{--}155 \text{ K}; 6 \text{ pts})$.

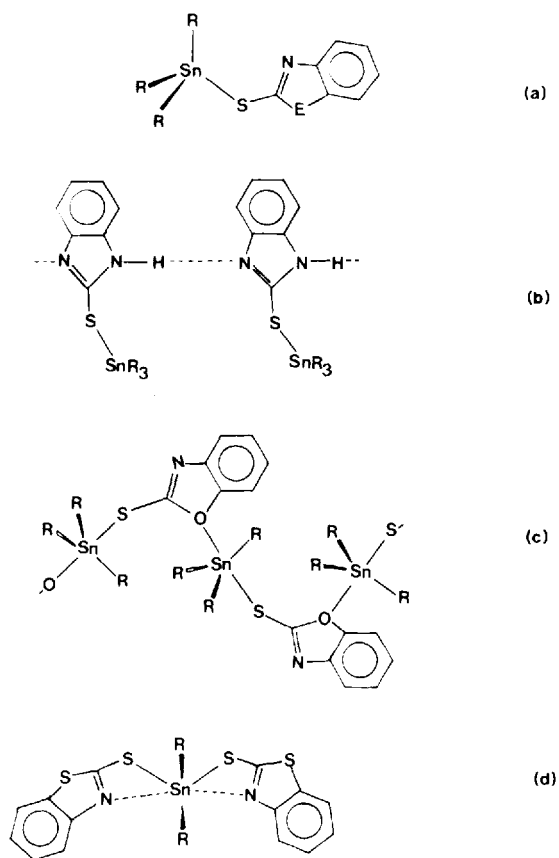


Figure 2 Proposed structures: (a) tetrahedral, monomeric adopted by all compounds except (b) $\text{Cy}_3\text{Sn(mbi)}$; (c) $\text{Bu}_3\text{Sn(mbo)}$ at 78 K and (d) $\text{Bu}_2\text{Sn(mbt)}_2$.

organotin compounds studied, save $\text{Bu}_3\text{Sn(mbo)}$, have QS values in the range $1.80\text{--}2.40 \text{ mm s}^{-1}$, and are again somewhat inconclusive in determining the coordination number at tin, since typically tetrahedral and *cis*- XYSnR_3 structures have associated QS values in the ranges $1.00\text{--}2.40$ and $1.70\text{--}2.40 \text{ mm s}^{-1}$ respectively.³⁷ QS data for $\text{Bu}_3\text{Sn(mbo)}$ (3.26 mm s^{-1}) is quite different, and is typical of a *trans*- XYSnR_3 geometry about tin. This can arise from covalent bonding to S coupled with a coordinate bond from either O or N of the heterocycle, the former seeming most likely since no similar behaviour arises for $\text{Bu}_3\text{Sn(mbt)}$. The resulting polymeric structure (Fig. 2c) is common for alkyltin derivatives of oxygenated ligands but less so for aryltin species³⁸ and the diminished Mössbauer QS data for $\text{Ph}_3\text{Sn(mbo)}$ would appear consistent with this trend. It must be remembered, however, that for $\text{Bu}_3\text{Sn(mbo)}$ the polymeric structure is only valid in the solid state (78 K) and not necessarily true for the room temperature oil. While we have been unable to synthesise a pure sample of $\text{Me}_3\text{Sn(mbo)}$ to extend the range of this polymeric structural type, similar structural changes for other room temperature oils have been noted, e.g. $\text{Me}_3\text{SnS}_2\text{P(OR)}_2$ ($\text{R} = \text{Et}, i\text{-Pr}$).³⁹

In the case of $\text{Bu}_2\text{Sn(mbt)}_2$ ($\text{QS} = 2.37 \text{ mm s}^{-1}$), the structural choice lies between a tetrahedral or six-coordinate R_2SnX_4 geometry about tin. $^2J(^{119}\text{Sn}\text{--}^{13}\text{C})$ of 505 Hz^{24} is too high for the former but in keeping with the latter, although the degree of distortion from four toward six

coordination must be small since we estimate the $\angle \text{C-Sn-C}$ from the QS data using the model of Bancroft and Sham⁴⁰ to be 109° , with errors in the model of ca. $\pm 13^\circ$ (Molloy, unpublished work). While these data cannot unambiguously specify whether distortions toward six-coordination yield *cis*- or *trans*- R_2Sn fragments, the latter (Fig. 2d) is almost always adopted by dialkyltin systems.³⁹ The Mössbauer spectrum of $\text{Bu}_2\text{Sn}(\text{mbt})_2$ also contains a small amount of a second doublet ($\text{IS}=1.00$, $\text{QS}=2.04 \text{ mm s}^{-1}$), which other authors²⁴ ascribe to a thione form of the ligand N-bonded to tin but with weak chelation via S to yield a *cis*- R_2SnX_4 coordination about the metal. We feel that an alternative, and more plausible rationale, is that this second component is due to unreacted Bu_2SnO ($\text{IS}=1.04$, $\text{QS}=2.09 \text{ mm s}^{-1}$).⁴¹

Variable-temperature ^{119}Sn Mössbauer data for two compounds, $\text{Cy}_3\text{Sn}(\text{mbt})$ and $\text{Cy}_3\text{Sn}(\text{mbi})$, are shown pictorially in Fig. 3. We and others⁴³ have shown that the slope of plots of $\text{Ln}A(T)$ vs T (normalisation to 78 K is merely to facilitate inter-sample comparison), i.e. $a = -d\text{Ln}(A)/dT$ reflect the tightness of binding of tin within the

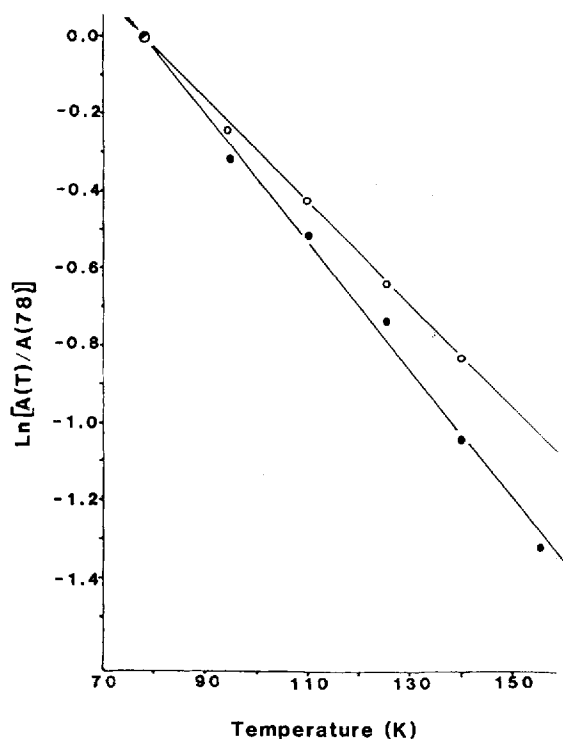


Figure 3 Variable-temperature ^{119}Sn Mössbauer spectroscopic data for $\text{Cy}_3\text{Sn}(\text{mbt})$ (○) and $\text{Cy}_3\text{Sn}(\text{mbi})$ (●).

solid lattice. The rigidity of the lattice as experienced by the Mössbauer atom depends upon (i) monomer vs polymer formation (ii) the strength of intermolecular interactions and (iii) the linearity of the polymer chain. More rigid lattices show shallower plots, that is lower values of $a \cdot 10^2 a$ for $\text{Cy}_3\text{Sn}(\text{mbt})$ (1.35 K^{-1}) is at the interface of data for weakly bridged 1-d polymers (e.g. Cy_3SnCl , $10^2 a = 1.40 \text{ K}^{-1}$; Cy_3Sn -1,2,4-triazole, $10^2 a = 1.31 \text{ K}^{-1}$) and monomeric species (e.g. Cy_4Sn , $10^2 a = 1.14 \text{ K}^{-1}$; Cy_3SnBr , $10^2 a = 1.60 \text{ K}^{-1}$), but in the light of other spectroscopic data presented above this data arises from non-interacting molecules rather than a weakly bridged polymer. Data for $\text{Cy}_3\text{Sn}(\text{mbi})$ ($10^2 a = 1.68 \text{ K}^{-1}$) rule out a polymeric structure centred on tin, but are consistent with $[\text{Cy}_3\text{Sn}]$ pendant to a chain structure based upon hydrogen bonded $\text{NH} \cdots \text{N}$ units (see infrared data), similar to the structure adopted by tricyclohexyltin-3-indolylacetate ($10^2 a = 1.75 \text{ K}^{-1}$) which we have recently reported.⁴⁴

While the spectroscopic evidence for structural assignments in the title systems is far from certain, the data as a whole suggest monomeric, tetrahedral species, all bonded to tin via S(exo) except (i) $\text{Bu}_3\text{Sn}(\text{mbo})$ which is a polymer in the solid state via S,O linkages, (ii) $\text{Cy}_3\text{Sn}(\text{mbi})$, in which the tetrahedral tin is pendant to a hydrogen bonded benzimidazole chain and (iii) $\text{Bu}_2\text{Sn}(\text{mbt})_2$ which is weakly six-coordinate via S(exo) and N chelation. These structures are each shown in Fig. 2.

The structure of S-(tricyclohexylstannyl)-2-mercaptobenzothiazole

In view of the uncertainties in structure assignments indicated above, we have determined the structure of $\text{Cy}_3\text{Sn}(\text{mbt})$ by x-ray crystallography. The asymmetric unit is shown in Fig. 4 and the unit cell contents in Fig. 5. Bond distances and angles are given in Table 3 and related structural data for comparison in Table 6. The structure confirms the linkage between tin and the benzothiazole as being via the exocyclic sulphur atom, and the geometry about tin is that of a distorted tetrahedron. The $\text{Sn} \cdots \text{N}$ distance is $3.055(8) \text{ \AA}$, which is within the sum of the respective van der Waal's radii (3.67 \AA), but is longer than other secondary $\text{N} \rightarrow \text{Sn}$ bonds, e.g. $\text{Me}_3\text{SnO}_2\text{CCH}_2\text{NH}_2$, 2.46 \AA ;⁴⁵ $\text{Bu}_2\text{Sn}(\text{SC}_5\text{H}_4\text{N}-2, \text{NO}_2-5)_2$, 2.77 \AA .⁴⁶ Moreover, the proximity of

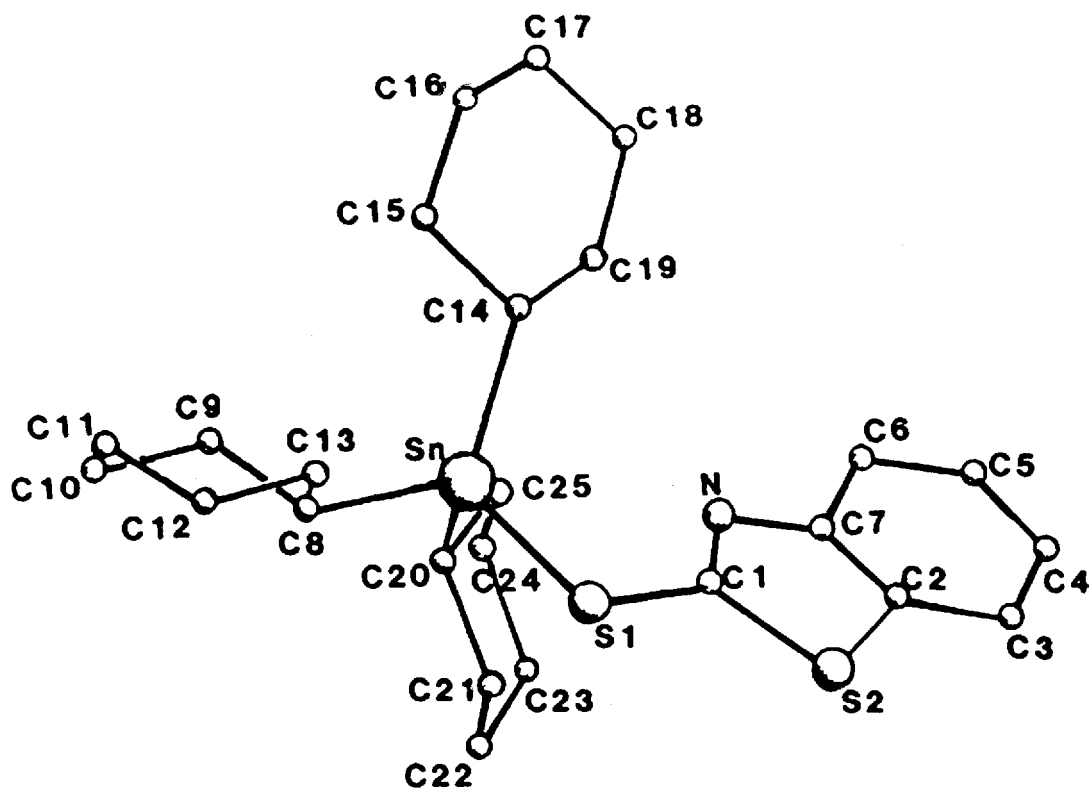


Figure 4 The asymmetric unit of $\text{Cy}_3\text{Sn}(\text{mbt})$ shown the atomic numbering scheme employed.

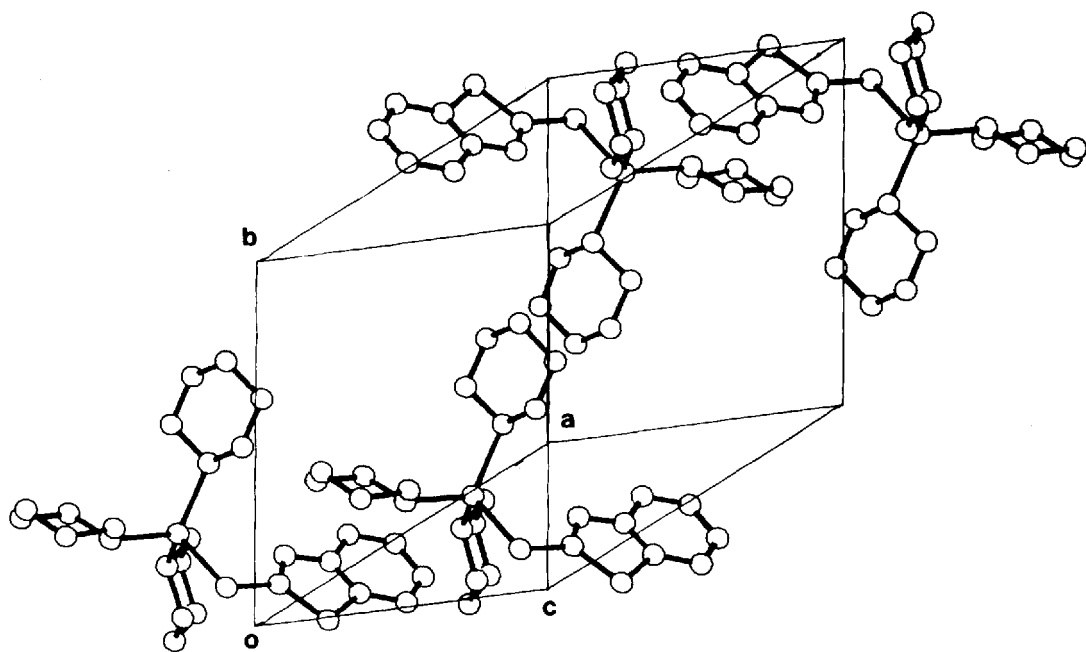


Figure 5 The unit cell of $\text{Cy}_3\text{Sn}(\text{mbt})$.

Table 6 Comparative bond length (Å) data for $\text{Cy}_3\text{Sn}(\text{mbt})$ and related compounds

Compound	Sn—S(1)	Sn—N	Sn—C(mean)	S(1)—C(1)	C(1)—N	Ref.
Hmbt	—	—	—	1.662	1.353	10
$\text{Cy}_3\text{Sn}(\text{mbt})$	2.472	3.055	2.167	1.743	1.290	This work
$\text{Ph}_3\text{SnSC}_6\text{H}_4\text{Bu}^i\text{-}p$	2.413	—	2.126	1.784	—	49
Ph_3SnSMe	2.391	—	2.137	1.770	—	50
$\text{Ph}_3\text{SnSC}_5\text{H}_4\text{N-}p$	2.567	2.62	—	—	—	51
$\text{Bu}_2\text{Sn}[2\text{-SC}_5\text{H}_3\text{N}(\text{NO}_2\text{-}5)]_2$	2.477	2.77	2.162	1.73	1.32	46
$\text{Co}(\text{mbt})_2(\text{py})_2$	—	—	—	1.706 ^a	1.312 ^a	18
$[\text{NEt}_4][\text{Cd}(\text{mbt})_3]$	—	—	—	1.693	1.303	3
$\text{Ru}_2(\text{mbt})_2(\text{py})_2(\text{CO})_4$	—	—	—	1.718 ^b	1.306 ^b	4
$\text{Ru}(\text{mbt})_2(\text{py})_2(\text{CO})_2$	—	—	—	1.724	1.287	5
$\text{Re}_2(\text{mbt})_2(\text{CO})_6$	—	—	—	1.76	1.25	6
$[\text{NBu}_4][\text{Zn}(\text{mbt})_3(\text{H}_2\text{O})]$	—	—	—	1.725 ^{b,c}	1.301 ^{b,c}	3
—	—	—	—	1.690 ^d	1.331 ^d	3
$[\text{NBu}_4][\text{Zn}(\text{mbt})(\text{dmt})_2]^{\text{e}} \cdot \text{EtOH}$	—	—	—	1.679 ^d	1.328 ^d	3
$[\text{NBu}_4][\text{Zn}(\text{mbt})_2(\text{dmt})]^{\text{e}}$	—	—	—	1.681 ^{b,d}	1.316 ^{b,d}	3

^aAverage for two independent molecules in asymmetric unit, ^bAverage for two ligands, ^cBonded to metal via S(1) only; N is H-bonded to H_2O . ^dMetal bonded via N only, ^edmt = dimethyl dithiocarbamate.

N to Sn does not cause any angular changes consistent with the formation of a *cis*- NSSnC_3 local geometry at tin. In such a structure, with C(8) and N in axial sites, the sum of angles at Sn between equatorial ligating atoms is 334.9° , compared to ideal tetrahedral and trigonal bipyramidal values of 328.5 and 360° respectively. The angular distortions away from tetrahedral are generally small, except C(8)—Sn—S(1) which closes to 96.6° . However a similar angle is found in $\text{Ph}_3\text{SnSC}_6\text{H}_4\text{Bu}^i\text{-}p$ (98.5°), so its origin lies in either electronic or crystal packing effects rather than a stereochemical interaction involving the ring nitrogen. The Sn—S and Sn—C bond lengths are unexceptional, and are similar to those found in related systems.

In its non-complexed form, Hmbt adopts a thione structure (I), i.e. the C(1)—S(1) bond (1.662Å) has mostly double bond character and the C(1)—N bond (1.353Å) is essentially a single bond. The structure of $\text{Cy}_3\text{Sn}(\text{mbt})$ shows that upon coordination to tin the ligand undergoes a redistribution of electron density towards the thiol structure (II). That is, the C(1)—S(1) bond lengthens (1.743Å) consistent with a decrease in bond order, though it is still shorter than S—C bonds in $\text{Ph}_3\text{SnSCH}_3$ (1.77Å) or $\text{Ph}_3\text{SnSC}_6\text{H}_4\text{Bu}^i\text{-}p$ (1.784Å). The C(1)—S(2) bond does not change upon complexation (1.734Å) and is largely of single bond character. The C(1)—N bond concomitantly shortens upon complexation from 1.353 to 1.29Å , with increasing

bond order. Coordination between ligand and metal via the exocyclic S only, as in $\text{Cy}_3\text{Sn}(\text{mbt})$ or $\text{Ru}(\text{mbt})_2(\text{py})_2(\text{CO})_2$ ⁵, is clearly shown by the thiol arrangement of bond lengths, while coordination by N only, as in $[\text{NBu}_4]^+[\text{Zn}(\text{mbt})(\text{S}_2\text{CNMe}_2)_2]^-$ is characterised by the thione bond length pattern. Chelation by N and S leads to intermediate C(1)—S(1) and C(1)—N bond lengths (e.g. $\text{Co}(\text{mbt})_2(\text{py})_2$: C(1)—S(1) 1.709 ; C(1)—N 1.304Å),¹⁸ consistent with delocalisation of the double bond character over the S—C—N residue.

There is no evidence for intermolecular bonding interactions (Fig. 5) thus clarifying the origin of the variable-temperature Mössbauer spectroscopic data as arising from packing effects rather than lattice association. Furthermore, from the crystallographic evidence for $\text{Cy}_3\text{Sn}(\text{mbt})$ the appearance of ditin fragments in the mass spectra of $\text{Bu}_3\text{Sn}(\text{mbt})$ and $\text{Me}_3\text{Sn}(\text{mbt})$ is made the more perplexing.

In view of the similarity of spectroscopic data for other triorganotin compounds studied, including $\text{Bu}_3\text{Sn}(\text{mbo})$ at room temperature, the coordination sphere about tin is likely to be very similar to that described above for $\text{Cy}_3\text{Sn}(\text{mbt})$.

Biocidal activity and comments on structure/activity relationships

Biological activity patterns for $\text{Ph}_3\text{Sn}(\text{mbo})$, $\text{Ph}_3\text{Sn}(\text{mbt})$ and $\text{Cy}_3\text{Sn}(\text{mbt})$ are given in Table 7. $\text{Cy}_3\text{Sn}(\text{mbt})$ shows the greatest pesticidal activity.

Table 7 Biocidal testing^a of Ph₃Sn(mbo), Ph₃Sn(mbt) and Cy₃Sn(mbt)^a

	Ph ₃ Sn(mbo)	Ph ₃ Sn(mbt)	Cy ₃ Sn(mbt)
Pesticidal activity ^b			
<i>Tetranychus urticae</i> (adults) (500 µg g ⁻¹)	—	5	9
LC _{50,90} (µg g ⁻¹)	—	50.2, 104.0	16.8, 39.6
<i>Chilo partellus</i>	—	—	9
LC _{50,90}	—	—	1332, 2829
<i>Musca domestica</i> LC _{50,90} (µg g ⁻¹)	—	—	660, 1000
Fungicidal activity ^c			
<i>Botrytis cinerea</i> (5 µg g ⁻¹)	0	0	—
<i>Puccinia recondita</i> (25, 5 µg g ⁻¹)	3, 0	2, —	—
<i>Venturia inaequalis</i> (25, 2.5 µg g ⁻¹)	3, 0	0, —	0, —
<i>Pyricularia oryzae</i> (50, 25 µg g ⁻¹)	4, 4	4, —	2, —
<i>Cercospora arachidicola</i> (25, 2.5 µg g ⁻¹)	4, 2	2, —	—
<i>Plasmopara viticola</i> (25, 1 µg g ⁻¹)	4, 2	4, 2	1, —
<i>Phytophthora infestans</i> (100 µg g ⁻¹)	2	1	1
<i>Rhynchosporium secalis</i> (25, 5 µg g ⁻¹)	3, 1	3, 0	0, —
<i>Pyrenophora teres</i> (25, 10 µg g ⁻¹)	4, 0	4, 0	1, —
<i>Septoria nodorum</i> (25 µg g ⁻¹)	1	2	0

^aConcentrations of organotin used in test are given in parentheses, ^bPesticidal activity is on a 0–9 scale where 0=0–49% kill, 5=50–79% kill and 9=80–100% kill, ^cFungicidal activity is on a 0–4 scale where 4=no disease, 3=trace–5%, 2=6–25%, 1=26–60% and 0=>60% disease.

ity of the three compounds tested and >80% kills were achieved at the 500 µg g⁻¹ (ppm) level against *Tetranychus urticae* (two spotted mite), *Nilaparvata lugens* (brown planthopper) and *Chilo partellus* (maize and sorghum stem borer). Against *Tetranychus*, LC_{50,90} levels were 16.8 and 39.6 ppm which corresponds to approximately half the activity of the commercially exploited tricyclohexyltin hydroxide (Plictran®). For comparison, the measured LC_{50,90} for Ph₃Sn(mbt) were 50.2, 104 ppm respectively. Against *Chilo partellus* and *Musca domestica* (housefly) LC₅₀ was at 1332 and 660 ppm for Cy₃Sn(mbt), which compares unfavourably with the contemporary organic pesticides, e.g. chlorpyrifos (Dursban®; ×0.01) and permethrin (Ambush®; ×0.03).

In fungicidal tests, the two triphenyltin compounds were noticeably more potent than Cy₃Sn(mbt), and of these Ph₃Sn(mbo) was the more active. Specifically for Ph₃Sn(mbo), >95% control was found against *Puccinia recondita* (brown rust), *Venturia inaequalis* (apple scab), *Pyricularia oryzae* (rice blast), *Cercospora arachidicola* (peanut leafspot), and *Plasmopara viticola* (vine downy mildew) at 25 ppm levels. At the 2.5–5.0 µg g⁻¹ level activity was lost against *Puccinia* and *Venturia*, while against *Cercospora* and

Plasmopara only 75–94% control remained at 1.0–2.5 µg g⁻¹ levels. Similar concentration/activity trends were noted against *Rhynchosporium secalis* (leaf blotch), *Pyrenophora teres* (net blotch) and *Septoria nodorum* (glume blotch), which in toto suggests that the activity of the organotin diminishes markedly at concentrations less than ca. 5.0 µg g⁻¹. For comparison, Cy₃Sn(mbt) was ineffective against *Venturia* at 25 µg g⁻¹, and achieved only 75–94% control against *Pyricularia* at 50 µg g⁻¹. Ph₃Sn(mbt) was inactive against *Venturia* (25 ppm) and *Botrytis cinerea* (grey mould) (5 µg g⁻¹), showed diminished activity compared to Ph₃Sn(mbo) against *Puccinia* and *Cercospora*, and a similar activity/concentration relationship to the benzoxazole against *Plasmopara*. For Ph₃Sn(mbo) and Ph₃Sn(mbt) against *Phytophthora infestans* (potato late blight) 6–25% and 26–60% disease was noted while the commercial product triphenyltin acetate (Brestan®) shows no disease at the same concentration (100 µg g⁻¹).³¹ In all the fungicidal studies, the activity was always protectant, and no systemic behaviour was noted in any of the tests.

In a series of tests against a broad range of crop and weed species, all three compounds showed poor herbicidal properties, with any ac-

tivity being of a post- rather than a pre-emergent nature.

These studies confirm the acaricidal (pesticidal) nature of tricyclohexyltin derivatives, while triphenyltin derivatives show greatest activity toward fungi. In view of the broad spectrum of tests carried out only general comments concerning structure activity relationships can be made. In particular, it is interesting that four-coordinate $\text{Cy}_3\text{Sn}(\text{mbt})$ compares favourably in comparison to $\text{Cy}_3\text{Sn}(\text{dppd})$, tris-(2-methyl-2-phenylpropyl)-tin(hf) and $\text{Cy}_3\text{Sn}(\text{hf})$ (dppd = 1,3-diphenylpropane-1,3-dione; hf = 3-hydroxyflavone) which show $< \times 0.1$ the activity at $> \times 5$ the concentration. Similarly, the two four-coordinate triphenyltin compounds $\text{Ph}_3\text{Sn}(\text{mbt})$ and $\text{Ph}_3\text{Sn}(\text{mbo})$ have broad spectrum fungicidal behaviour, and in particular show ca. $\times 0.75$ the activity of $\text{Ph}_3\text{SnO}_2\text{CCH}_3$ against *Phytophthora infestans*, while the five-coordinate $\text{Ph}_3\text{Sn}(\text{hf})$, $\text{Ph}_3\text{Sn}(\text{qo})$ and $\text{Ph}_3\text{Sn}(\text{qt})$ (qo = 8-hydroxyquinoline; qt = 8-mercaptoquinoline) show $< \times 0.5$ the control.³¹ Our findings thus concur with the postulates made previously that five coordinate tin, in either a *trans*- X_2SnR_3 ⁴⁷ or a *cis*- X_2SnR_3 ⁴⁸ is less active in general than four-coordinate R_3SnX compounds, although the *trans*- X_2SnR_3 shows increasing activity at lower concentrations as the polymer chain breaks up to yield a coordination number of four at tin. This dependence on coordination number could arise either from the lability of the anion towards formation of $\text{R}_3\text{Sn}(\text{H}_2\text{O})_2^+$, or if coordination saturation at tin inhibits the further binding of N,O,S donor groups of biological macromolecules.

Acknowledgements We thank ICI Plant Protection Division (Jealotts Hill) for carrying out the testing of these compounds and their permission to publish the results. We would also like to acknowledge the National Institute for Higher Education (Dublin) where this work was initiated, and Dr S.J. Blunden (International Tin Research Institute, Uxbridge) for recording the ^{119}Sn n.m.r. data.

REFERENCES

1. Ashworth, CC, Bailey, NA, Johnson, M, McCleverty, JA, Morrison, N and Tabbiner, B *J. Chem. Soc., Chem. Commun.*, 1976, 743
2. McCleverty, JA, Morrison, NJ, Spencer, N, Ashworth, CC, Bailey, NA, Johnson, MR, Smith, JMA, Tabbiner, BA and Taylor, CR *J. Chem. Soc., Dalton Trans.*, 1980, 1945
3. McCleverty, JA, Gill, S, Kowalski, RSZ, Bailey, NA, Adams, H, Lumbard, KW, and Murphy, MA, *J. Chem. Soc., Dalton Trans.*, 1982, 493
4. Jeannin, S, Jeannin, Y and Lavigne, G *Trans. Met. Chem.*, 1976, 1: 186
5. Jeannin, S, Jeannin, Y, and Lavigne, G *Trans. Met. Chem.*, 1976, 1: 192
6. Jeannin, S, Jeannin, Y and Lavigne, G *Trans. Met. Chem.*, 1976, 1: 195
7. Belen-Kii, SM USSR Patent 162, 738; *Chem. Abs.*, 1964, 61: P11691c
8. Patel, NK, Makwana, SC and Patel, MM *Corrosion Sci.*, 1974, 14: 91
9. Owens, RG 1969. Organic Sulphur Compounds. In: *Fungicides: an Advanced Treatise*. Torgeson, DC (ed.) Vol. II, Academic Press, New York, 1969, pp. 147
10. Chesick, JP and Donohue, J *Acta Cryst.*, 1971, B27: 1441
11. Form, GR, Raper, ES and Downie, TC *Acta Cryst.*, 1976, B32: 345
12. Banerji, S, Byrne, RE and Livingstone, SE *Trans. Met. Chem.*, 1982, 7: 5
13. Koleva, EG *Comptes Rend. Acad. Bulg. Sci.*, 1980, 33: 1663
14. El-Shazly, MF, Salem, T, El-Sayed, MA and Hedewy, S *Inorg. Chim. Acta*, 1978 29: 155
15. Khullar, IP and Agarwala, U *Can. J. Chem.*, 1975, 53: 1165
16. Dehand, J and Jordanov, J *Inorg. Chim. Acta*, 1976, 17: 37
17. Srivastava, SK, Gupta, A and Verman, A *Egypt. J. Chem.*, 1983, 23: 173
18. Dance, IG and Isaac, D *Aust. J. Chem.*, 1977, 30: 2425
19. Molloy, KC and Purcell, TG *J. Organomet. Chem.*, 1986, 312: 167.
20. Ison, RR, Newbold, GT and Sagggers, DT *Pest. Sci.*, 1971, 2: 152
21. Czerwinska, E, Eckstein, Z, Ejmocki, Z and Kowalik, R *Bull. Acad. Pol. Sci. Ser. Sci. Chim.*, 1967, 15: 335
22. Stapfer, CH *J. Paint Tech.*, 1969, 41: 309
23. Domazetis, G, Majee, RJ and James, BD *J. Organomet. Chem.*, 1978, 148: 339
24. Domazetis, G, Majee, RJ, James, BD and Cashion, JD *J. Inorg. Nucl. Chem.*, 1981, 43: 1351
25. Molloy, KC, Purcell, TG, Quill, K and Nowell, I *J. Organomet. Chem.*, 1984, 267: 237
26. Main, P, Fiske, SE, Hull, SL, Germain, G, Declercq, JP and Wollfson, MM Multan: a System of Computer Programs for Crystal Structure Determination from X-ray Diffraction Data. Universities of York (UK) and Louvain (Belgium), 1980
27. Sheldrick, GM *SHELX a computer Program for Crystal Structure Determination*, University of Cambridge (UK), 1976
28. Cromer, DT and Mann, JB *Acta Cryst.*, 1968, A24: 321
29. Stewart, RF, Davidson, ER and Simpson, WT *J. Chem. Phys.*, 1965, 42: 3175
30. Cromer, DT and Liberman, DJ *J. Chem. Phys.*, 1970, 53: 1891
31. Blunden, SJ, Smith, PJ and Sugavanam, B *Pestic. Sci.*, 1984, 15: 253

-
32. Fish, RH, Holmstead, RL and Casida, JE *Tet. Lett.*, 1974, 14: 1303
 33. Devillanova, FA and Verani, G *Aust. J. Chem.*, 1980, 33: 279
 34. George, TA *J. Organomet. Chem.*, 1971, 31: 233
 35. Harrison, PG *Inorg. Chem.*, 1973, 12: 1545
 36. Blunden, SJ and Hill, R *Inorg. Chim. Acta*, 1985, 98: 1.7–L8
 37. Davies, AG and Smith, PJ Tin. In: *Comprehensive Organometallic Chemistry*, Wilkinson, G, Stone, FGA and Abel, EW (eds) 1982, Chapter 11, p. 525
 38. Cusack, PA, Smith, PJ, Donaldson, JD and Grimes, SM *International Tin Research Institution (London)*, 1981, Publication 588
 39. Lefferts, JL, Molloy, KC, Zuckerman, JJ, Haiduc, I, Guta, C and Ruse, D *Inorg. Chem.*, 1980, 19: 1662
 40. Bancroft, GM and Sham, TK *Inorg. Chem.*, 1975, 14: 2281
 41. Ruddick, JNR *Rev. Silicon, Germanium, Tin and Lead Compounds*, 1976, II: 115
 42. Molloy, KC and Quill, K *J. Chem. Soc., Dalton Trans.*, 1984, 1417
 43. Harrison, PG, Phillips, RC and Thornton, EW *J. Chem. Soc., Chem. Commun.*, 1977, 603
 44. Molloy, KC, Purcell, TG, Hahn, E, Schumann, H and Zuckerman, JJ *Organometallics*, 1986, 85
 45. Ho, BYK, Molloy, KC, Zuckerman, JJ, Reidinger, F and Zubieta, JA *J. Organomet. Chem.*, 1980, 187: 213
 46. Domazetis, G, James, BD, Mackay, MF and Magee, RJ *J. Inorg. Nucl. Chem.*, 1979, 41: 1555
 47. Ascher, KR and Nemny, NE *Experimentia*, 1976, 32: 902
 48. Tzschach, A, Weichmann, H and Jurkschat, K *J. Organomet. Chem. Libr.*, 1981, 12: 293
 49. Clarke, PL, Cradwick, ME and Wardell, JL *J. Organomet. Chem.*, 1973, 63: 279
 50. Andreetti, BD, Bocelli, G, Calestani, G and Sgarabotto, P *J. Organomet. Chem.*, 1984, 273: 31
 51. Bokii, NG, Struckov, Yu T, Kravtsov, TN and Rokhlina, EM *J. Struct. Chem.*, 1973, 14: 458